A&A 656, L1 (2021)
https://doi.org/10.1051/0004-6361/202039752

Astronomy & Astrophysics
Special issue

Solar Orbiter First Results (Cruise Phase)

LETTER TO THE EDITOR

^{3}He-rich solar energetic particle events observed on the first perihelion pass of Solar Orbiter

G. M. Mason[1], G. C. Ho[1], R. C. Allen[1], J. Rodríguez-Pacheco[2], R. F. Wimmer-Schweingruber[3], R. Bučík[4], R. Gómez-Herrero[2], D. Lario[5], J. L. F. von Forstner[3], G. B. Andrews[1], L. Berger[3], I. Cernuda[2], F. Espinosa Lara[2], W. J. Lees[1], C. Martin[3,6], D. Pacheco[3], M. Prieto[2], S. Sánchez-Prieto[2], J. R. Hayes[1], C. E. Schlemm[1], H. Seifert[1], and K. Tyagi[1,7]

[1] Johns Hopkins Univ. Applied Physics Laboratory, Laurel, MD, USA
e-mail: glenn.mason@jhuapl.edu
[2] Space Research Group, Universidad de Alcalá, Alcalá de Henares, Spain
[3] Institut für Experimentelle und Angewandte Physik, Christian-Albrechts-Universität zu Kiel, Kiel, Germany
[4] Southwest Research Institute, San Antonio, TX, USA
[5] NASA Goddard Space Flight Center, Greenbelt, MD, USA
[6] German Aerospace Center (DLR), Berlin, Germany
[7] Univ. Colorado/LASP, Boulder, CO, USA

Received 23 October 2020 / Accepted 14 November 2020

ABSTRACT

We report observations of five impulsive solar energetic particle (SEP) events observed inside 1 au during the first perihelion pass of the Solar Orbiter mission, which was launched in February 2020. These small events were all reasonably associated with active regions observed from Earth but which had rotated out of view by the time of the Solar Orbiter observations. Even though most of the events were small, their spectral forms, ^{3}He content, and association with type III bursts convincingly identifies them as ^{3}He-rich impulsive SEP events with properties similar to those previously observed at 1 au. Three of the events showed fast ion rise times, and two of them had long-lasting anisotropies consistent with the Compton-Getting effect.

Key words. acceleration of particles – Sun: abundances – Sun: flares – Sun: particle emission

1. Introduction

Solar energetic particle (SEP) events are of broad interest since they can fill the interplanetary medium with high energy radiation which may affect the Earth and assets in space. The events begin with the explosive release of magnetic energy in or near the solar corona, which accelerates particles by a number of mechanisms, notably shock waves and magnetic reconnection. A prime goal of the Solar Orbiter mission (Müller et al. 2020) is to better understand the physical processes operating in SEP events by observing them from closer distances to better observe the source and to sample fields and particles in situ before many details are washed out in the interplanetary medium.

In the current solar minimum, large shock-associated SEP events are nearly absent, and none were detected by Solar Orbiter during the first half year after launch. However, impulsive SEP events were observed. This class of small events is associated with soft X-ray emission, type III radio bursts and energetic particles, and often with enhanced ^{3}He and heavy ions, which appear to originate in the lower corona in association with emerging magnetic flux regions near coronal holes, with particle injection accompanied by extreme ultraviolet (EUV) plasma jets (e.g., reviews by Reames 1999; Wang et al. 2006; Mason 2007; Bučík 2020). Because of their low intensities, observing them closer to the Sun is obviously advantageous in seeking to pinpoint the sources and mechanisms responsible. This Letter reports five such events observed on Solar Orbiter and discusses their properties and implications for future studies; as the payload becomes fully commissioned, the perihelion moves closer to the Sun, and solar activity increases.

2. Observations

The observations reported here were made with the Suprathermal Ion Spectrograph (hereafter SIS), which is one of several sensors in the Energetic Particle Detector (EPD) suite (Rodríguez-Pacheco et al. 2020). SIS is a time-of-flight mass spectrometer that measures the ion composition from H through ultra-heavy nuclei over the energy range of ~0.1−10 MeV/nucleon. SIS has two telescopes, one facing sunward (telescope a), and the other anti-sunward (b). Figure 1 (left) shows the orbital position of Solar Orbiter from the launch on 9 Feb. 2020 through 1 Oct. 2020 with locations of the SEP events and the location of STEREO-A which provided type III radio burst information. The right panel shows suprathermal H and Fe intensities; the Fe intensities were chosen from a lower energy to provide better statistics. During this period, the SEP events stand out from other particle events, which are associated with corotating interaction regions, by their higher intensity, short duration, and relatively high Fe content (Allen et al. 2021).

Table 1 lists the details of the events. We now discuss the specific details of each event.

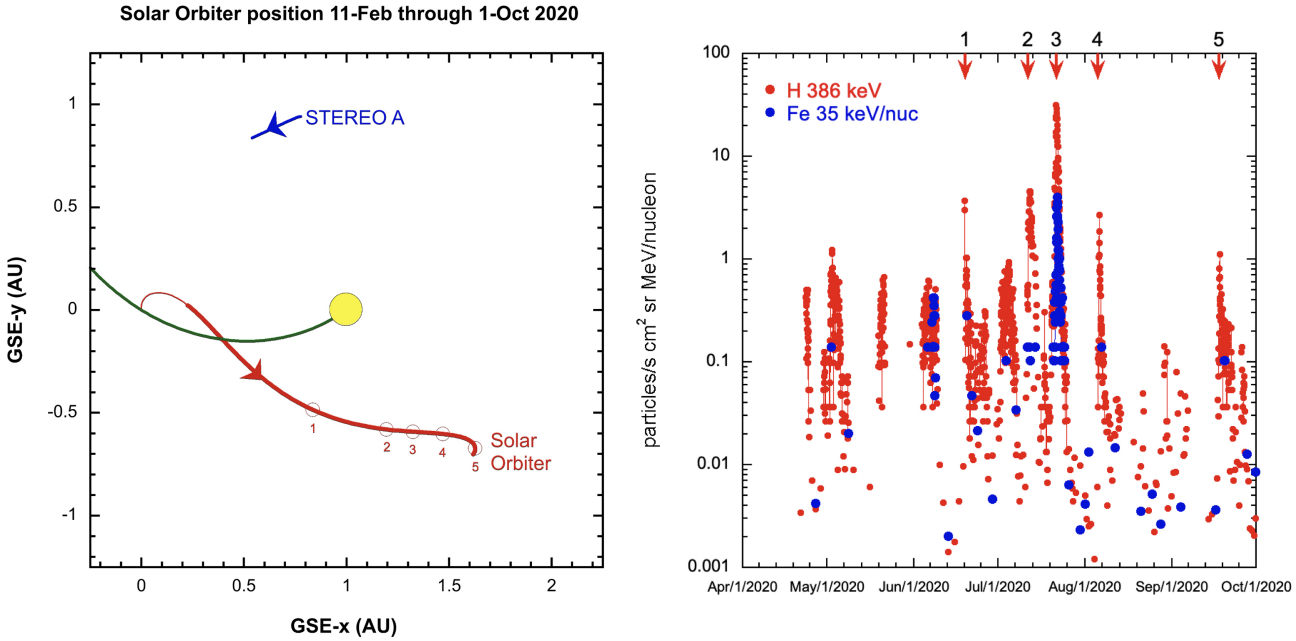

Fig. 1. *Left*: Solar Orbiter position from launch through 1 Oct. 2020 (red curve). The period after SIS turn-on is shown in a thick line along with the spacecraft position at each of the five observed SEP events; the green Parker spiral line corresponds to a 400 km s^{-1} solar wind speed. *Right*: suprathermal H and Fe intensities showing the five SEP events.

Table 1. ^{3}He-rich solar energetic particle event properties.

Event	1	2	3	4	5
Estimated injection	18 Jun. (170)	11 Jul. (193)	20 Jul. (202)	5 Aug. (218)	17 Sep. (261)
Time [(1)]	13:15	02:25	20:15 [(2)]	17:00	09:40
Angle (deg) [(3)]	W 68.7	W 107	W 117	W 126	W 130
Footpoint (deg) [(4)]	102	209	95.1	262	75.9
Dist. (au) [(5)]	0.52	0.61	0.67	0.78	0.96
Lat. (deg) [(6)]	−1.51	2.88	0.74	−2.08	−5.97
Active region [(7)]	12765	12767	12768	12271	12773
AR-footpoint angle (deg) [(8)]	11	12	18	35	7
^{4}He fluence [(9)] $\times 10^3$	0.52 ± 0.11	1.67 ± 0.19	174 ± 2	4.8 ± 0.3	1.8 ± 0.2
^{3}He/^{4}He [(10)]	0.1 ± 0.1	0.15 ± 0.06	0.61 ± 0.01	0.05 ± 0.01	0.04 ± 0.04
H spectral index [(11)]	−4.3	−3.7	−2.2	−1.0	−3.0
^{4}He spectral index [(11)]	−4.5	−3.2	−2.2	−1.3	−3.4
Fe spectral index [(11)]	…	…	−2.7	…	…
35 keV electrons inj.? [(2)]	Yes	…	Yes	Yes	Yes

Notes. [(1)]Year: 2020; Event 1: based on weak type III (STEREO-A); Event 2: type III STEREO-A; Event 3: multiple type IIIs, the largest was chosen; Event 4: no type III was seen based on the rise at SO; Event 5: a possible feature in STEREO-A SWAVES. [(2)]See Gómez-Herrero et al. (2021); for Event 3 there appears to be a second injection corresponding to a type III burst at day 203 02:55. [(3)]The separation angle from Earth (deg). [(4)]In Carrington longitude, assuming a 300 km s^{-1} solar wind speed typical of slow solar wind streams in 2020 observed on ACE. [(5)]Solar Orbiter heliocentric distance (au). [(6)]Solar Orbiter heliographic latitude (deg). [(7)]NOAA Active Regions observed from Earth. [(8)]Approximate angular separation of AR from nominal footpoint (deg). [(9)]Particles cm^{-2} sr MeV/nucleon at 385 keV/nucleon. [(10)]Energy range 0.5–2.0 MeV/nucleon. [(11)]In the range 0.1–1.0 MeV/nucleon.

2.1. 18 Jun. 2020 event

Figure 3 (top left) shows this event's sharp onset when the spacecraft entered a flux tube that was still being filled with injected particles showing large (~20:1 telescope a:b ratio) anisotropies. Following this, the intensities dipped as the magnetic field line moved away from the telescope fields of view, then they recovered and continued for more than a day with sustained (~3:1) anisotropies. There was a possible presence of ^{3}He, but Fe was not detected.

2.2. 11 Jul. 2020 event

This event's onset was associated with a jet beyond the west limb observed from near Earth by the NASA Solar Dynamics Observatory Atmospheric Imaging Assembly. The jet's brightness peaked at around 02:20–02:22 UT in coincidence with the type III burst; however, the jet was in the northern hemisphere and AR 12767 was at ~S20, so the jet may might not be associated with the type III burst and presumed injection for the ^{3}He-rich event. Although intensities remained low, the event continued

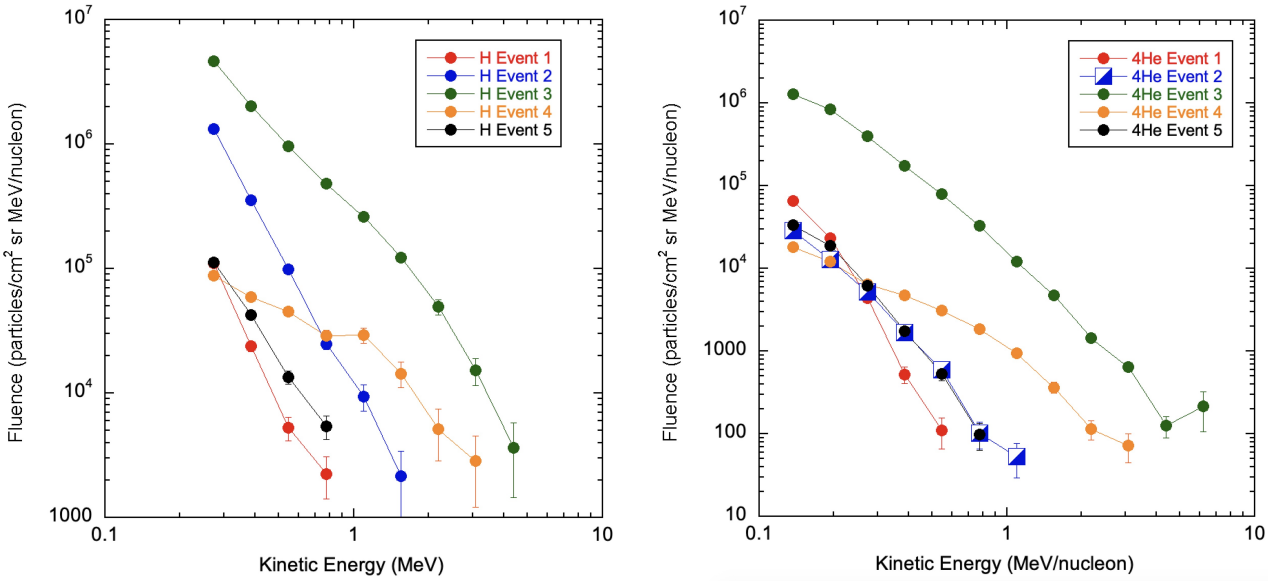

Fig. 2. *Left*: proton fluence spectra. *Right*: helium fluence spectra for each SEP event.

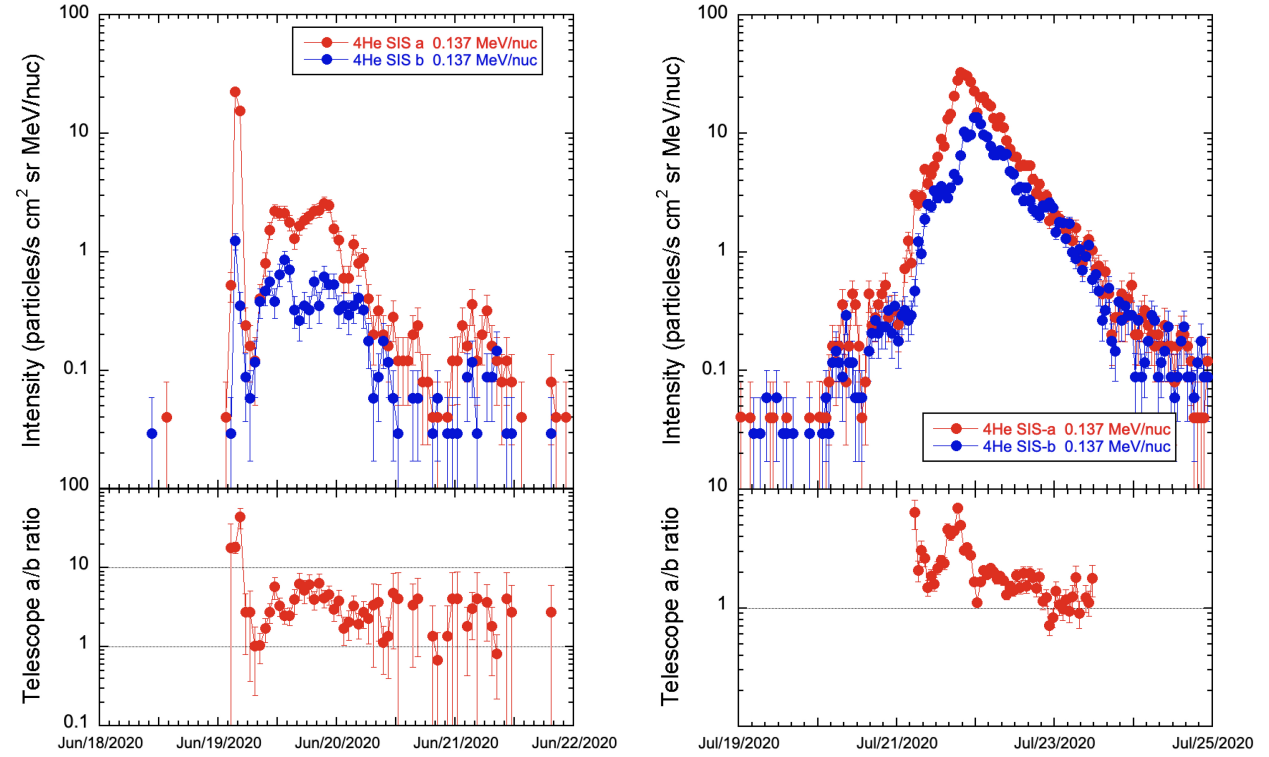

Fig. 3. *Top panels*: 137 keV/nucleon ^{4}He for (*left*) the 19 Jun. 2020 and (*right*) 21 Jul. 2020 events. Sunward intensities are red circles and anti-sunward intensities are blue circles. *Bottom panels*: ratio of sunward and anti-sunward He intensities.

for about 3 days during which the anisotropies remained near 2:1, but with poor statistical accuracy. In addition to H and ^{4}He, SIS measured ^{3}He, O, and enhanced Fe in this event.

2.3. 20 Jul. 2020 event

Precursor intensity increases with ^{3}He:^{4}He ~1 began about 30 hr before this event's onset, accompanied by multiple type III bursts along with multiple jets observed over the east limb by STEREO EUVI. During the initial rise phase, the ^{3}He:^{4}He ratio remained near 1, then around 12:00 on 21 Jul. 2020, H and ^{4}He intensities rose again, probably due to a second injection associated with a strong type III burst early on 21 July 2020. Energetic electrons (>30 keV) were detected by the EPD STEP sensor with at least two separate rises consistent with multiple ion injections (Gómez-Herrero et al. 2021). Figure 3 (right) shows that even though the intensity rise in this event was slow, anisotropies reached ~5:1 then decayed closer to ~2:1 until almost a day after the maximum, then they remained small thereafter. This event was more than an order of magnitude more intense than the others, permitting statistically accurate measurements of the composition (see Appendix A).

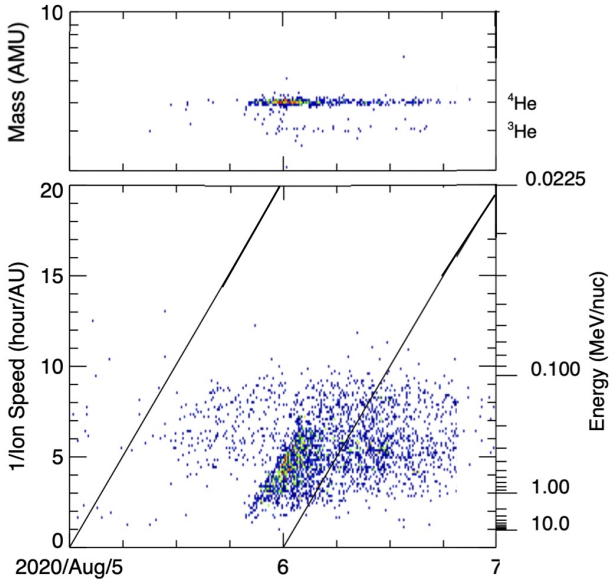

Fig. 4. *Upper panel*: mass arrival spectrogram for 0.4−10 MeV/nucleon. *Lower panel*: 1/v versus arrival time for H and heavier ions; slanted lines show arrival times for 300 km s^{-1} solar wind and 0.78 au.

2.4. 5 Aug. 2020 event

Figure 4 shows spectrograms for ^{3}He and ^{4}He (upper panel) and ion arrival times (lower panels) with clear velocity dispersion consistent with a solar injection around 17:00 on 5 Aug. 2020. No type III bursts were seen by STEREO. Energetic electrons were observed in association with this event. The H and He spectra roll over at lower energies (Fig. 2), making this the hardest spectrum of the set. There were a few O counts around 100 keV/nucleon, but not enough to form a spectrum.

2.5. 17 Sep. 2020 event

At the time of this weak event, Solar Orbiter had moved out to nearly 1 au. There was a weak radio burst, possibly a type III burst, which preceded the dispersionless particle rise by a few hours. The event had modest anisotropy at the peak, and there was some evidence of ^{3}He. Too few heavy ions were detected to form spectra.

3. Conclusions

Even though the observations presented here were taken during solar minimum conditions, Solar Orbiter observed several impulsive events during its first perihelion pass, each reasonably associated with an active region detected earlier or later from Earth. Several such events were also observed with ACE instruments during the 2007−2008 solar minimum (Mason et al. 2009). However, during the period studied here, we note that ACE observed no impulsive ion events at 1 au. A major goal of Solar Orbiter in studies of impulsive events is to better understand the source regions, propagation, and composition by observing closer to the Sun where timing uncertainties decrease and higher fluences permit more accurate measurements. Very close to the Sun, it may be possible to approach a long standing question regarding the clear association of type III events with ^{3}He-rich events (Reames et al. 1988; Ho et al. 2001; Wang et al. 2012), which is whether numerous, closely spaced type III events are each associated with a ^{3}He ion injection, which is masked at 1 au, since there is too much mixing during transport to 1 au. This may give insight into whether the acceleration of the ions and electrons is from the same location, or whether they originate in different locations. Closer to the Sun, the higher fluences should allow for significantly improved studies on ultraheavy nuclei in these events, whose intensities at 1 au are so low that they can only be sampled by summing multiple events (Reames 2000; Mason et al. 2004).

The current set of events has properties similar to previous observations at 1 au. The nearly scatter-free keV electron profiles often observed with these events has led to modeling, which assumes that the ion injection duration is short, on the duration of hours (Mason et al. 1989; Wang et al. 2005). The long-lasting anisotropies observed in Events 1 and 3 are consistent with estimates of the Compton-Getting effect (Appendix B).

In this first perihelion pass of Solar Orbiter, many instruments were still being commissioned. Therefore, the full set of supporting measurements, such as radio, EUV, X-ray, and solar wind, that will be available for future studies will be critical for placing our energetic particle observations in the context required to make decisive advances in understanding these events.

Acknowledgements. The Suprathermal Ion Spectrograph (SIS) is a European facility instrument funded by ESA. The SIS instrument was constructed by the JHU/Applied Physics Lab. and CAU Kiel. We thank the many individuals at ESA and within the Energetic Particle Detector team for their support in its development. Post launch operation of SIS at APL is funded by NASA contract NNN06AA01C, and we thank NASA headquarters and the NASA/GSFC Solar Orbiter project office for their continuing support. The UAH team acknowledges the financial support by the Spanish Ministerio de Ciencia, Innovación y Universidades FEDER/MCIU/AEI Projects ESP2017-88436-R and PID2019-104863RB-I00. The CAU Kiel team thanks the German Federal Ministry for Economic Affairs and Energy and the German Space Agency (Deutsches Zentrum für Luftund Raumfahrt, e.V., (DLR)) for their unwavering support under grant numbers 50OT0901, 50OT1202, and 50OT1702; and ESA for supporting the build of SIS under contract number SOL.ASTR.CON.00004, and the University of Kiel and the Land Schleswig-Holstein for their support of SIS. We acknowledge data from the STEREO SWAVES website, the ACE website, and the Solar Orbiter magnetometer team on the Solar Orbiter Archive (SOAR). We thank the referee for helpful comments.

References

Allen, R. C. G., Mason, G. M., Ho, G. C., et al. 2021, A&A, 656, L2 (SO Cruise Phase SI)
Bučík, R. 2020, Space Sci. Rev., 216, A24
Desai, M. I., Mason, G. M., Gold, R. E., et al. 2006, ApJS, 649, 470
Gómez-Herrero, R., Pacheco, D., Kollhoff, A., et al. 2021, A&A, 656, L3 (SO Cruise Phase SI)
Ho, G. C., Roelof, E. C., Hawkins, S. E., III, et al. 2001, ApJ, 552, 863
Ipavich, F. M. 1974, Geophys. Res. Lett., 1, 149
Mason, G. M. 2007, Space Sci. Rev., 130, 231
Mason, G. M., Ng, C. K., Klecker, B., & Green, G. 1989, ApJ, 339, 529
Mason, G. M., Wiedenbeck, M. E., Miller, J. A., et al. 2002, ApJS, 574, 1039
Mason, G. M., Mazur, J. E., Dwyer, J. R., et al. 2004, ApJS, 606, 555
Mason, G. M., Nitta, N. V., Cohen, C. M. S., & Wiedenbeck, M. E. 2009, ApJ, 700, L56
Müller, D., St Cyr, O. C., Zouganelis, I., Gilbert, H. E., & Marsden, R. 2020, A&A, 642, A1
Reames, D. V. 1999, Space Sci. Rev., 90, 413
Reames, D. V. 2000, ApJS, 540, L111
Reames, D. V., Dennis, B., Stone, R., & Lin, R. P. 1988, ApJ, 327, 998
Rodríguez-Pacheco, J., Wimmer-Schweingruber, R. F., Mason, G. M., et al. 2020, A&A, 642, A7
Wang, L., Lin, R. P., Krucker, S., & Mason, G. M. 2005, in Proceedings of the Solar Wind 11/SOHO 16, eds. B. Fleck, T. H. Zurbuchen, & H. Lacoste, 457
Wang, Y.-M., Pick, M., & Mason, G. M. 2006, ApJ, 639, 495
Wang, L., Lin, R. P., Krucker, S., & Mason, G. M. 2012, ApJS, 759, 69

Appendix A: 21 July 2020 event composition

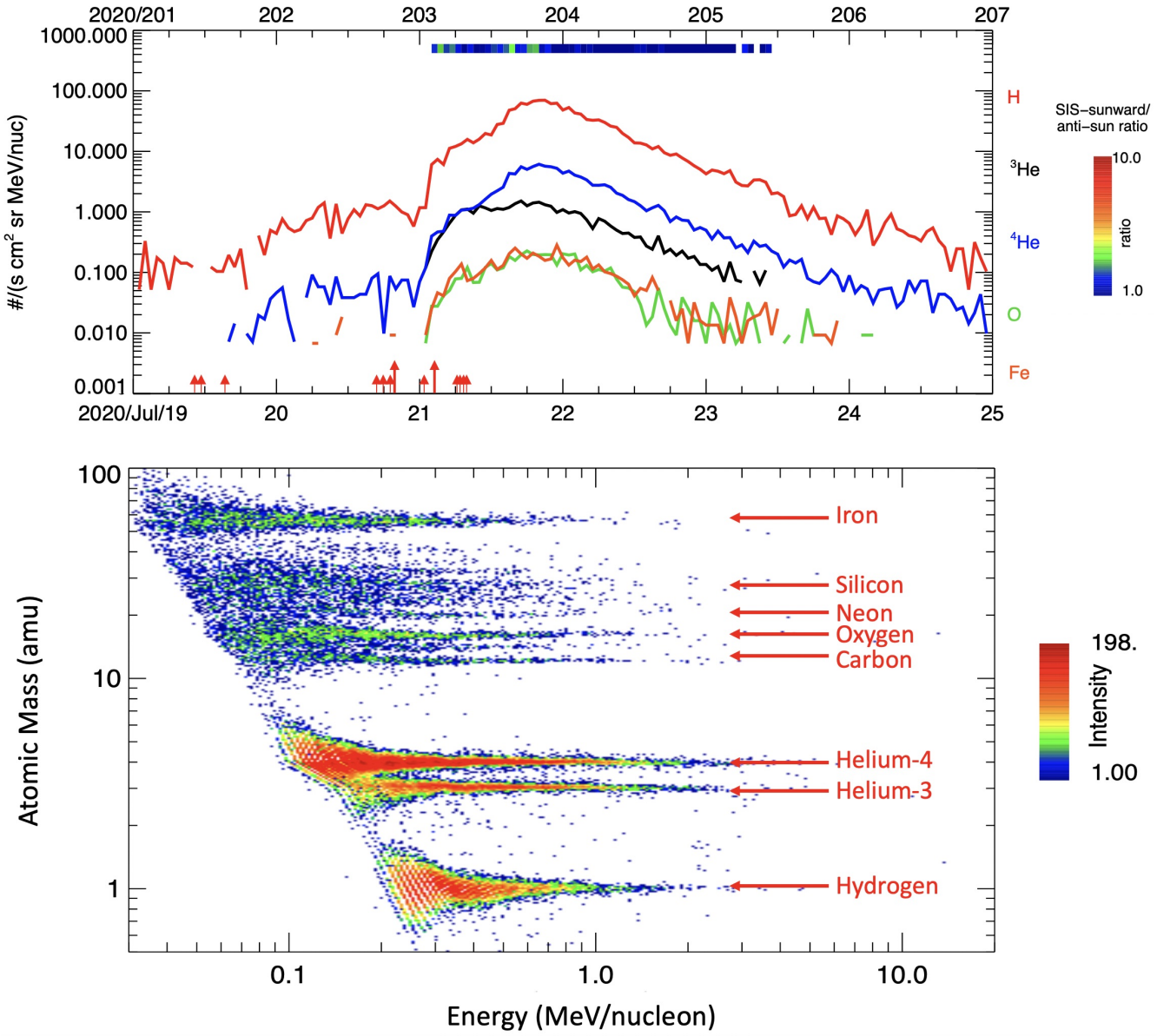

Fig. A.1. *Top*: particle intensities for the 21 Jul 2020 event. Red arrows mark the times of type III bursts seen on STEREO. *Bottom*: mass spectrogram.

The upper panel of Fig. A.1 shows time-intensity profiles of the 21 Jul. 2020 event, which occurred when the spacecraft was at 0.67 au. The intensities rose above the background ~1–2 days before the event, with large enrichments of ^{3}He, and multiple type III events. The large intensity rise is associated with stronger type III events late on 20 July 2020 and early on 21 July 2020. It appears that both caused particle injections, and keV electron observations from EPD also showed at least two injections (for more details see Gómez-Herrero et al. 2021). We note that the ^{3}He is equal to ^{4}He early in the event, then H and ^{4}He increase further around day 203.6 presumably from the second injection. The lower panel is a mass spectrogram for the event, with major ion tracks that are clearly visible. It is important to note the large abundance of Fe in the spectrogram, with Fe/O ratio of 0.57 ± 0.05 at 385 keV/nucleon. This enhanced Fe/O is in the typical range for ^{3}He-rich events.

Particle spectra and the He mass histogram are in Fig. A.2. The spectral rollovers toward low energy (left) are often seen in these events at 1 au (Mason et al. 2002). The He mass histogram (right) yields a ^{3}He:^{4}He ratio 0.61 ± 0.01 in the range of 0.5–2.0 MeV/nucleon. Toward lower energies, the ^{3}He spectrum hardens compared to ^{4}He, so the ratio decreases; this feature has often been seen at 1 au. Relative abundances at 385 keV/nucleon are listed in Table A.1 and are close to surveys at a comparable energy (Mason et al. 2004) and at ~2.5 MeV/nucleon (Reames 1999). The table also lists the average abundances for large coronal mass ejection (CME)-associated SEP events in the SIS energy range from the survey of Desai et al. (2006). It can be seen from the table that the 21 Jul. 2020 event shows enrichment in heavy ions typically seen in ^{3}He-rich events.

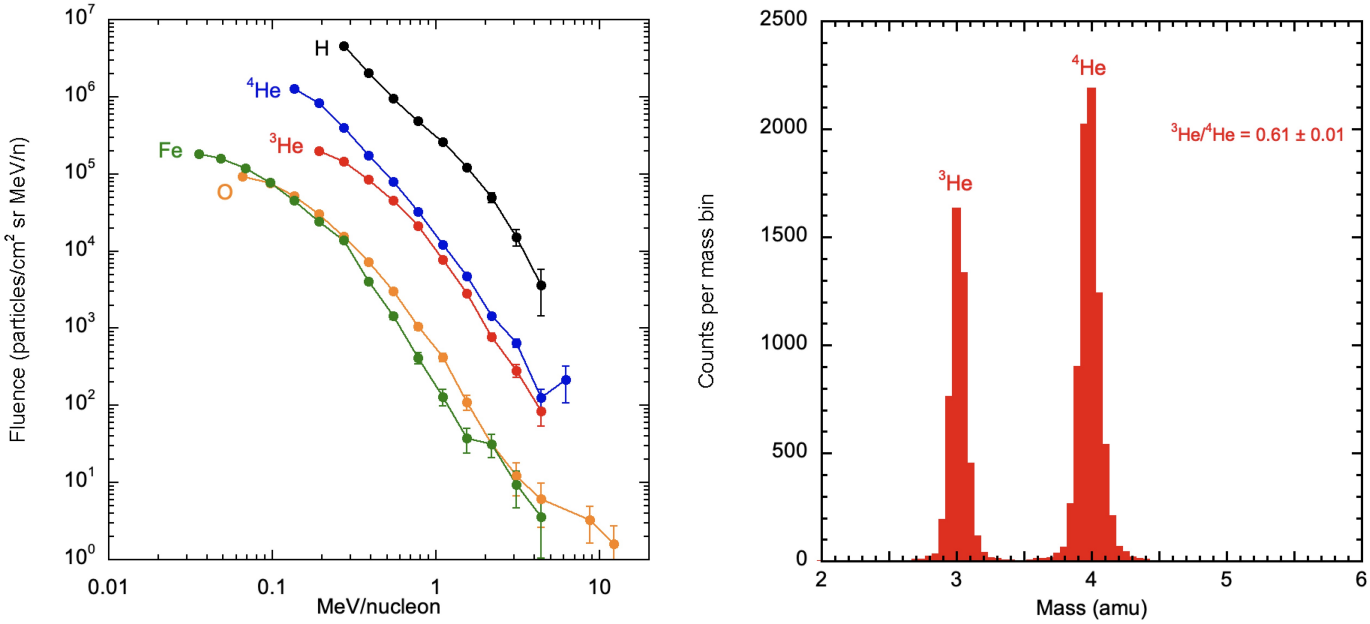

Fig. A.2. *Left*: fluences for selected species in the 21 Jul. 2020 event. *Right*: mass histograms for 0.5−2.0 MeV/nucleon He.

Table A.1. SEP abundances (O ≡ 1).

Species	21 July 2020 [(1)]	Large SEP Survey [(2)]
^{4}He	34.33 ± 0.093	75.0 ± 23.6
C	0.467 ± 0.002	0.361 ± 0.012
N	0.240 ± 0.001	0.119 ± 0.003
O	≡1.000 ± 0.004	≡1.00 ± 0.02
Ne	0.284 ± 0.002	0.152 ± 0.005
Mg	0.297 ± 0.002	0.229 ± 0.007
Si	0.317 ± 0.002	0.235 ± 0.011
S	0.112 ± 0.001	0.059 ± 0.004
Ca	0.058 ± 0.001	0.022 ± 0.002
Fe	0.738 ± 0.003	0.404 ± 0.047

Notes. [(1)]This work. [(2)]0.38 MeV/nucleon, Desai et al. (2006).

Appendix B: Compton-Getting estimates

Figure B.1 shows the ratios of the sunward and anti-sunward (a/b) telescope intensities for ^{4}He for several energy ranges. The ratios were calculated during later portions of the events when the a/b ratios were roughly steady (Event 1, 19 Jun. 2020 10:00−22:00; Event 3, 22 July 2020 02:00−20:00). Compton-Getting anisotropies (Ipavich 1974) were calculated using spectral indices from Table 1, and solar wind speeds were chosen to provide values that are close to the lower energy points (375 km s^{-1} for 10 June 2020; 300 km s^{-1} for 21 July 2020).

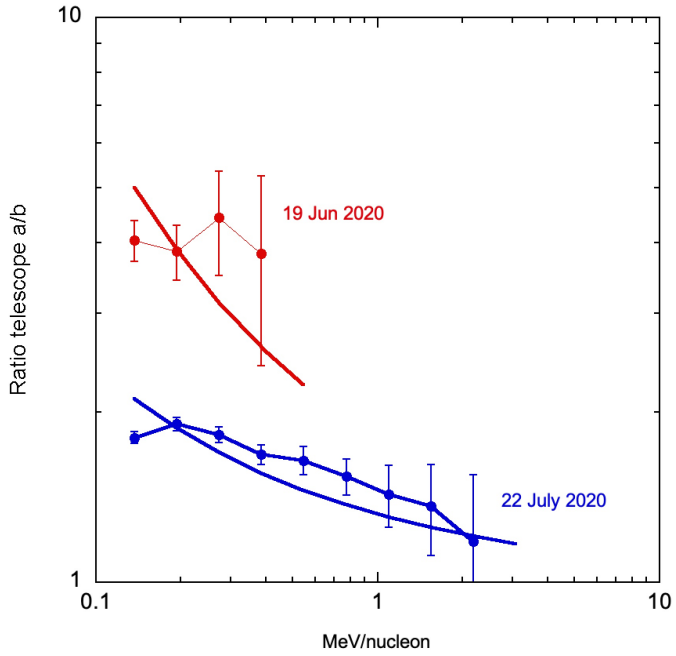

Fig. B.1. Sunward and anti-sunward telescope intensities for ^{4}He (filled circles) and estimated Compton-Getting anisotropies (solid lines).